
RITUAL: Random Image Transformations as a Universal Anti-hallucination Lever in LVLMS

Sangmin Woo* Jaehyuk Jang* Donguk Kim* Yubin Choi Changick Kim
KAIST

{smwoo95, jhyuk, kdu3613, choibinbin, changick}@kaist.ac.kr

<https://sangminwoo.github.io/RITUAL/>

Abstract

Recent advancements in Large Vision Language Models (LVLMS) have revolutionized how machines understand and generate textual responses based on visual inputs. Despite their impressive capabilities, they often produce "hallucinatory" outputs that do not accurately reflect the visual information, posing challenges in reliability and trustworthiness. Current methods such as contrastive decoding have made strides in addressing these issues by contrasting the original probability distribution of generated tokens with distorted counterparts; yet, generating visually-faithful outputs remains a challenge. In this work, we shift our focus to the opposite: What could serve as a complementary enhancement to the original probability distribution? We propose a simple, training-free method termed **RITUAL** to enhance robustness against hallucinations in LVLMS. Our approach employs random image transformations as complements to the original probability distribution, aiming to mitigate the likelihood of hallucinatory visual explanations by enriching the model's exposure to varied visual scenarios. Our empirical results show that while the isolated use of transformed images initially degrades performance, strategic implementation of these transformations can indeed serve as effective complements. Notably, our method is compatible with current contrastive decoding methods and does not require external models or costly self-feedback mechanisms, making it a practical addition. In experiments, **RITUAL** significantly outperforms existing contrastive decoding methods across several object hallucination benchmarks, including POPE, CHAIR, and MME.

1 Introduction

Large Vision-Language Models (LVLMS) [1, 6, 27, 28, 54] have emerged as a pivotal technology, enabling machines to interpret complex visual scenes and generate contextually appropriate textual descriptions. These models integrate and process inputs from both visual and linguistic domains, offering unprecedented possibilities in applications ranging from video content creation [2] to assistive technologies [31, 37]. Despite their potential, LVLMS are often criticized for generating "hallucinatory" content [14, 24, 40, 51] — outputs that appear plausible but do not faithfully reflect the visual inputs. This gap in reliability and trustworthiness is particularly concerning for sensitive applications such as medical diagnosis [29, 52], surveillance [12, 43], and autonomous driving [23].

The challenge primarily arises from the difficulty in maintaining alignment between the visual inputs and textual outputs, given the complexity of training such models to accurately interpret and narrate visual data. Although several strategies have been developed to mitigate these issues, they often require extensive additional training [11, 16, 26, 30, 36, 39, 45, 47, 48, 53], sophisticated feedback mechanisms [17, 36, 45, 46], or reliance on auxiliary models [7, 21, 38, 44, 50], which can complicate deployment and scalability.

*Equal Contribution

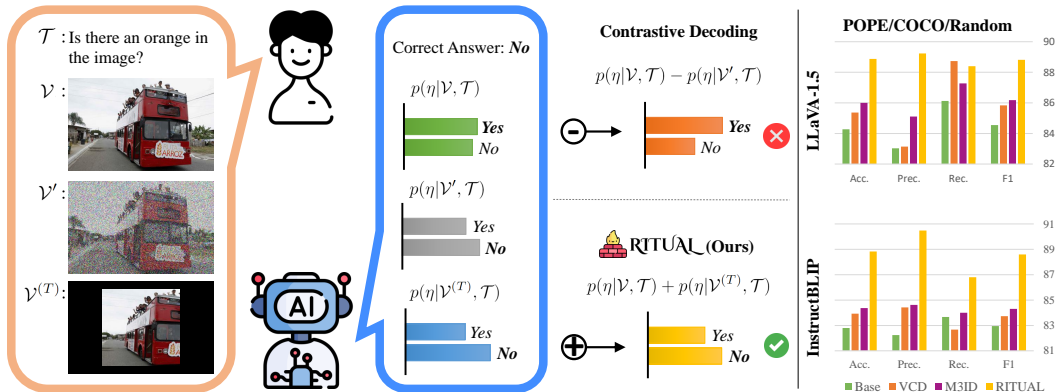


Figure 1: **An illustration of RITUAL** Unlike contrastive decoding methods [9, 19], which contrast the conditional probability given the original image (\mathcal{V}) to that given a diffused [19] (or absent [9]) image (\mathcal{V}'), we leverage both the original image (\mathcal{V}) and a randomly transformed image ($\mathcal{V}^{(T)}$) in a complementary manner. While simple, RITUAL achieves state-of-the-art performance on multiple hallucination benchmarks, including the POPE [24].

Contrastive decoding [9, 19, 41], a notable approach in this context, refines the model outputs by contrasting the conditional probability of textual responses given the original visual input versus a distorted visual input. This aims to alleviate language biases or statistical priors, ensuring that responses are more grounded in the actual images, thereby reducing deviations from the visual truth. While beneficial, contrastive decoding does not fully resolve the misalignments between visual data and textual descriptions and can sometimes lead to the reinforcement of incorrect patterns.

We present a simple, training-free approach termed RITUAL which leverages random image transformations to complement the original probability distributions of textual responses. Our method is distinct from contrastive decoding [9, 19, 41], which attributes the causes of hallucinations to language bias or statistical priors. Instead, RITUAL suggests that the source of hallucinatory content might actually reside within the images themselves, advocating for a multifaceted view of visual inputs. The conceptual comparison is shown in Fig. 1.

RITUAL is designed to address the issue of visual hallucination by employing a dual-input strategy that integrates both the original and a randomly transformed image. This provides a more comprehensive visual context, enriching the model’s exposure to a diverse array of visual scenarios, thereby enhancing the robustness and reliability of text generation. By integrating transformed versions of images during the decoding process, LVM can gain additional visual context that helps maintain the integrity of visual details in textual outputs.

It is important to note that these image transformations are not used in the training phase. As demonstrated in Fig. 2, using transformed images alone as visual input initially degrades performance compared to using the original image due to the introduction of novel visual artifacts. However, the combination of the original and transformed image significantly enhances the quality and reliability of the model’s outputs. While neither an original image nor a transformed image alone may provide an accurate response, their combination can reduce the likelihood of a hallucinated response and increase the likelihood of a correct answer.

In our experiments, RITUAL evaluates against several benchmarks, including POPE [34], CHAIR [24], and both MME-Hallucination and MME-Fullset from [10]. While maintaining simplicity, RITUAL effectively reduces hallucination across these benchmarks and enhances the general capability of LVMs. Notably, RITUAL surpasses existing contrastive decoding baselines [9, 19] in all tested benchmarks. RITUAL is also compatible with current contrastive decoding methods, and when used in conjunction, it further amplifies the improvements over these methods.

2 Related Work

Large Vision Language Models (LVLMs). Recent approaches to integrating visual and language modalities in LVLMs commonly leverage pre-trained uni-modal models. They include an adaptive interface to bridge pre-trained visual encoders with Large Language Models (LLMs), facilitating efficient information synthesis across modalities. These interfaces generally fall into two main

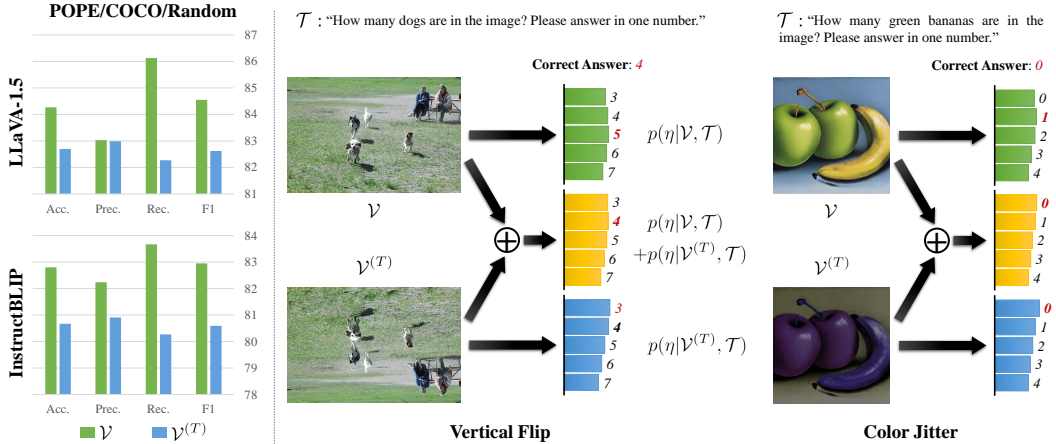


Figure 2: **Intriguing impact of random image transformations on LVLMs.** (Left) Using the randomly transformed image ($\mathcal{V}^{(T)}$) as a visual input to LVLMs [6, 28] results in lower performance compared to using the original image (\mathcal{V}). (Right) However, when these two images are combined, an intriguing phenomenon is observed: cases incorrectly predicted with the original image are now correctly predicted. (i) Although $\mathcal{V}^{(T)}$ alone does not yield a correct answer, it reduces the likelihood of a hallucinated answer and increases the likelihood of a correct answer. (ii) In some cases, $\mathcal{V}^{(T)}$ strongly aligns with the correct answer, leading to accurate answers.

categories: (1) *Learnable query-based methods*, exemplified by Q-Former [20] in InstructBLIP [6] and MiniGPT-4 [54], a set of learnable query tokens is employed to capture visual signals through cross-attention. These tokens are optimized to distill the essential visual information and input it into the LLM for further processing. (2) *Projection layer-based methods*, such as LLaVA [27, 28] and Shikra [3], use a linear projection layer to transform visual features into the input space of LLMs. This mapping ensures seamless integration between pre-trained visual representations and the LLMs, enabling the latter to interpret the visual content effectively. Both strategies translate visual features into formats that the LLMs can understand. Despite their efficacy, LVLMs still encounter challenges with hallucination, which we aim to mitigate in this work. We specifically use two representative models, LLaVA and InstructBLIP, for experiments.

Hallucinations in LVLMs. LVLMs are susceptible to visual hallucinations, in which the generated text descriptions include objects or details entirely irrelevant from the given image. A range of methods has been introduced to address the issue by additional training [11, 16, 26, 30, 36, 39, 45, 47, 48, 53]. While these approaches offer promise, they often face practical limitations due to their dependence on additional data and extensive training periods. In response to these limitations, training-free approaches have gained traction. These models aim to refine the model output by self-feedback correction [18, 45], providing additional knowledge using auxiliary models [7, 17, 38, 44, 50], and contrastive decoding [9, 19, 41, 49], which refines the generated outputs by contrasting the conditional probability of the original image with the distorted image. Our work adopts a unique approach by applying random image transformations to complement the original image. This provides a wide range of visual contexts, aiming to mitigate hallucinatory visual explanations without the complexities of extra models, additional training, or data requirements.

3 Approach: RITUAL

We present a simple decoding method that can be applied on-the-fly during token generation. Our method is training-free, does not require external models or a costly self-feedback mechanism, and remains compatible with existing contrastive decoding techniques [9, 19]. An overview of our method is illustrated in Fig. 3.

3.1 LVLN Formulation

Vision-Language Alignment. LVLN takes a visual input and a textual query as inputs, where the visual input provides contextual visual information to assist the model in generating a relevant response to the textual query. Initially, a vision encoder (e.g., ViT [8], CLIP [33], etc.) processes

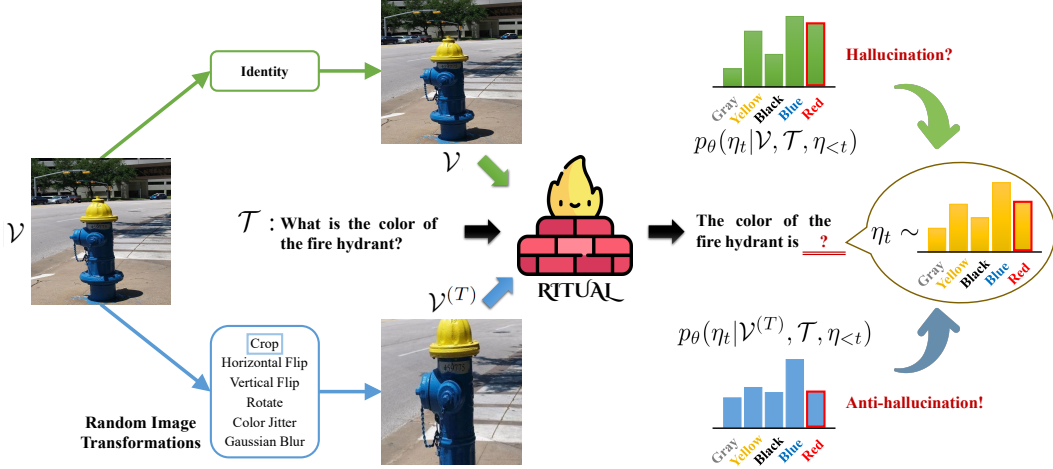


Figure 3: **Overview of RITUAL**. At each timestep t , LVLM auto-regressively samples a response η_t given a visual input, a textual query \mathcal{T} , and previously generated tokens $\eta_{<t}$. When conditioned on the original image \mathcal{V} , the probabilities for **Blue** (*correct*) and **Red** (*hallucinated*) responses are similar, which can lead to the hallucinated response being easily sampled. RITUAL leverages an additional probability distribution conditioned on the transformed image $\mathcal{V}^{(T)}$, where the likelihood of hallucination is significantly reduced. Consequently, the response is sampled from a linear combination of the two probability distributions, ensuring more accurate and reliable outputs.

raw images to extract visual features. These features are then projected into the language model’s input space using a vision-language alignment module (*e.g.*, Q-Former [20], linear projection [28], *etc.*), resulting in a set of visual tokens, $\mathcal{V} = \{\nu_0, \nu_1, \dots, \nu_{N-1}\}$. Concurrently, the textual inputs are tokenized into $\mathcal{T} = \{\tau_N, \tau_{N+1}, \dots, \tau_{N+M-1}\}$. The visual and textual tokens are concatenated to form an input sequence of length $N + M$.

Model Forwarding. The LVLM, parametrized by θ , processes the concatenated sequence of visual and textual tokens. This process is formalized as:

$$\mathcal{H} = \text{LVLM}_\theta([\mathcal{V}, \mathcal{T}]), \quad (1)$$

where \mathcal{H} denotes the sequence of output hidden states from the final layer of LVLM. These hidden states \mathcal{H} are used to compute the logits (or probabilities) for predicting the next tokens.

Response Generation. The LVLM generates responses auto-regressively, employing a causal attention mask to ensure each subsequent token is predicted based solely on the preceding tokens. Each response token is generated by sampling from the following probability distribution:

$$\eta_t \sim p_\theta(\eta_t | \mathcal{V}, \mathcal{T}, \eta_{<t}). \quad (2)$$

where η_t denotes the response token being generated at timestep t , and $\eta_{<t}$ indicates the sequence of tokens generated up to timestep $(t - 1)$. This generative process is iteratively continued, appending each newly predicted token to the sequence, until the termination of the sequence. By default, Greedy Decoding is used. Alternatively, decoding strategies such as Beam Search [42], Nucleus Sampling [13], or DoLa [5] can be employed.

3.2 Mitigating Visual Hallucinations in LVLM

Visual hallucinations in LVLM can occur during the decoding phase when tokens are selected based on erroneous probability distributions that do not align with the visual inputs. Our approach aims to mitigate these visual hallucinations with a simple yet effective modification to the input handling.

We first randomly apply common image transformations (*e.g.*, Crop, Flip, Color jitter, *etc.*) to the original visual input \mathcal{V} , This results in a transformed version of the visual input, $\mathcal{V}^{(T)}$.

$$\mathcal{V}^{(T)} = T(\mathcal{V}; \omega), \text{ where } \omega \in \Omega. \quad (3)$$

Here, T represents a specific transformation function selected randomly from a set of common image transformations (*e.g.*, Crop, Flip, Color Jitter, *etc.*). The parameter ω represents the specific

parameters of the transformation, drawn from a distribution Ω that governs the selection and nature of the transformation applied.

During the decoding phase, rather than using $\mathcal{V}^{(T)}$ alone — which we found to impair performance — we utilize both the original and transformed images. This dual-input approach significantly reduces the likelihood of hallucinatory outputs, as illustrated in Fig. 2, and improves the accuracy of the model’s predictions. The sampling equation in Eq. (2) is updated as follows:

$$\eta_t \sim p_\theta(\eta_t|\mathcal{V}, \mathcal{T}, \eta_{<t}) + \alpha p_\theta(\eta_t|\mathcal{V}^{(T)}, \mathcal{T}, \eta_{<t}). \quad (4)$$

Here, α is a balancing hyperparameter, adjusting the contribution of the transformed input relative to the original. To promote output diversity and avoid deterministic behavior, we choose to sample from a multinomial distribution rather than merely selecting the most probable output via argmax.

4 Experiments

4.1 Evaluation Setup

Throughout our experiments, we set hyperparameter configuration at $\alpha = 3$. For random image transformation, we use flip (horizontal & vertical), rotate, color jitter, Gaussian blur, and crop. In all experimental tables, the *base* refers to the standard decoding, which directly samples the response token from the softmax distribution.²

LVLMS. We integrate `RITUAL` with two state-of-the-art LVLMS: **LLaVA-1.5** ([28]) and **Instruct-BLIP** [6]. Both models incorporate Vicuna 7B [4] as their language decoding mechanism. LLaVA-1.5 utilizes linear projection layers to align image and text modalities and InstructBLIP employs the Q-Former [20] to efficiently bridge visual and textual features using a fixed number of tokens (*e.g.*, 32). Note that the adaptability of `RITUAL` extends beyond these two models and is model-agnostic. It can be compatible with a wide range of off-the-shelf LVLMS.

Baselines. Our method aims to reduce hallucinations in LVLMS without requiring external models, costly self-feedback mechanisms, or additional training. Therefore, we select baseline methods that align with these criteria. Recent contrastive decoding methods meet these requirements, and we establish two primary approaches as our baselines: **VCD** [19] and **M3ID** [9]. Both VCD and M3ID aim to mitigate object hallucinations by increasing the influence of the reference image over the language prior. This is achieved by contrasting output distributions derived from both original and distorted visual inputs. We reproduced VCD and M3ID within our evaluation setting.

Benchmarks. (1) **POPE** [24] frames hallucination assessment as a binary classification task using yes/no questions about object presence (*e.g.*, "Is there a dog in the image?"). It evaluates 500 MS-COCO images with questions based on actual objects or nonexistent objects. The benchmark contains three subsets (random, popular, and adversarial), addressing object prevalence and co-occurrences. (2) **MME** [10] is a comprehensive LVM benchmark assessing 14 subtasks, including object hallucination through tasks like object existence, count, position, and color. These tasks are framed as binary yes/no questions. (3) **CHAIR** [34] evaluates the proportion of words in captions that correspond to actual objects in an image, using ground-truth captions and object annotations. It has two variants: (i) per-sentence (CHAIR_S) is defined as $|\{\text{sentences with hallucinated objects}\}|/|\{\text{all sentences}\}|$. (ii) per-instance (CHAIR_I) is defined as $|\{\text{hallucinated objects}\}|/|\{\text{all objects mentioned}\}|$. We randomly select 500 images from the COCO [25] validation set and conduct image captioning with the prompt "Please describe this image in detail".

4.2 Results

Results on POPE. Table 1 compares various decoding-based hallucination mitigation methods on the POPE benchmark [24], evaluated with two representative LVLMS: LLaVA 1.5 [28] and Instruct-BLIP [6]. The results demonstrate that `RITUAL` consistently outperforms baseline and both VCD [19] and M3ID [9] across all datasets (MS-COCO [25], A-OKVQA [35], and GQA [15]) and setups (random, popular, and adversarial), and all metrics, demonstrating its robustness in mitigating hallucinations. This underscores the importance of considering visual context from multiple perspectives.

²We refer readers to the Appendix for further implementation/experimental details and additional results.

Setup	Method	LLaVA 1.5 [28]				InstructBLIP [6]				
		Acc. ↑	Prec. ↑	Rec. ↑	F1 ↑	Acc. ↑	Prec. ↑	Rec. ↑	F1 ↑	
MS-COCO [25]	Random	<i>base</i>	84.13	82.86	86.07	84.43	82.80	82.24	83.67	82.95
		VCD	85.37	83.14	88.73	85.84	83.93	84.42	82.67	83.73
		M3ID	86.00	85.11	87.27	86.18	84.37	84.62	84.00	84.31
		RITUAL	88.87	89.23	88.40	88.81	88.83	90.48	86.80	88.60
		RITUAL+VCD	89.07	89.49	88.53	89.01	89.30	90.85	87.40	89.09
		RITUAL+M3ID	89.00	89.85	87.93	88.88	88.93	91.13	86.27	88.63
	Popular	<i>base</i>	80.87	78.23	85.53	81.72	75.80	72.74	82.53	77.33
		VCD	81.10	77.78	87.07	82.16	77.73	75.43	82.27	78.70
		M3ID	82.83	79.62	88.27	83.72	77.30	74.10	83.93	78.71
		RITUAL	85.83	84.17	88.27	86.17	81.97	78.90	87.27	82.87
		RITUAL+VCD	85.77	83.89	88.53	86.15	82.83	80.16	87.27	83.56
		RITUAL+M3ID	85.37	83.60	88.00	85.74	81.90	78.98	86.93	82.77
	Adversarial	<i>base</i>	76.23	71.75	86.53	78.45	75.40	71.60	84.20	77.39
		VCD	75.60	70.78	87.20	78.14	76.80	73.62	83.53	78.26
		M3ID	77.70	73.23	87.33	79.66	76.03	72.48	83.93	77.79
		RITUAL	78.80	74.43	87.73	80.54	78.73	74.57	87.20	80.39
		RITUAL+VCD	79.60	75.26	88.20	81.22	79.07	74.89	87.47	80.69
		RITUAL+M3ID	79.20	74.83	88.00	80.88	78.93	75.06	86.67	80.45
A-OKVQA [35]	Random	<i>base</i>	81.73	76.53	91.53	83.36	81.13	78.03	86.67	82.12
		VCD	81.83	75.74	93.67	83.76	82.00	79.38	86.47	82.77
		M3ID	83.57	77.86	93.80	85.09	82.33	77.81	90.47	83.66
		RITUAL	85.17	79.79	94.20	86.40	87.13	83.92	91.87	87.71
		RITUAL+VCD	85.10	79.93	93.73	86.28	86.77	83.57	91.53	87.37
		RITUAL+M3ID	85.93	80.62	94.60	87.06	87.17	84.35	91.27	87.67
	Popular	<i>base</i>	76.67	70.51	91.67	79.71	75.67	70.97	86.87	78.12
		VCD	74.70	68.12	92.87	78.59	76.50	71.69	87.60	78.85
		M3ID	76.80	70.20	93.13	80.06	75.60	70.40	88.33	78.36
		RITUAL	78.83	71.99	94.40	81.68	78.73	72.83	91.67	81.17
		RITUAL+VCD	79.17	72.40	94.27	81.90	78.83	72.75	92.20	81.33
		RITUAL+M3ID	79.63	72.83	94.53	82.27	79.20	73.42	91.53	81.48
	Adversarial	<i>base</i>	67.40	61.78	91.27	73.68	68.00	63.08	86.80	73.06
		VCD	67.43	61.48	93.33	74.13	70.67	65.24	88.47	75.10
		M3ID	68.10	61.99	93.60	74.58	69.57	64.21	88.40	74.39
		RITUAL	68.57	62.26	94.27	74.99	70.27	64.15	91.87	75.55
		RITUAL+VCD	68.80	62.48	94.13	75.11	71.00	64.72	92.33	76.10
		RITUAL+M3ID	68.77	62.42	94.33	75.13	69.30	63.43	91.13	74.80
GQA [15]	Random	<i>base</i>	81.23	75.42	92.67	83.16	79.93	76.73	85.93	81.07
		VCD	81.50	74.78	95.07	83.71	81.83	79.03	86.67	82.67
		M3ID	82.83	76.64	94.47	84.62	80.57	76.77	87.67	81.85
		RITUAL	86.10	80.30	95.67	87.31	84.87	82.52	88.47	85.39
		RITUAL+VCD	86.03	80.21	95.67	87.26	84.97	82.40	88.93	85.54
		RITUAL+M3ID	86.30	80.64	95.53	87.46	85.00	82.94	88.13	85.46
	Popular	<i>base</i>	72.50	65.85	93.47	77.27	72.73	68.14	85.40	75.80
		VCD	71.57	64.72	94.80	76.93	73.67	68.82	86.53	76.67
		M3ID	72.83	66.04	94.00	77.58	74.57	69.45	87.73	77.53
		RITUAL	74.80	67.50	95.67	79.15	74.50	69.17	88.40	77.61
		RITUAL+VCD	75.07	67.82	95.40	79.28	75.33	69.98	88.73	78.25
		RITUAL+M3ID	74.40	67.15	95.53	78.87	75.57	70.24	88.73	78.41
	Adversarial	<i>base</i>	67.63	61.68	93.13	74.21	69.57	64.80	85.67	73.79
		VCD	67.47	61.38	94.20	74.33	69.43	64.76	85.27	73.61
		M3ID	68.13	61.88	94.47	74.78	68.90	64.06	86.13	73.47
		RITUAL	68.23	61.75	95.80	75.10	70.17	64.76	88.47	74.78
		RITUAL+VCD	69.00	62.39	95.67	75.53	70.23	64.81	88.53	74.84
		RITUAL+M3ID	68.80	62.29	95.27	75.33	71.00	65.32	89.53	75.53

Table 1: **Results on POPE [24] benchmark.** RITUAL consistently outperforms the contrastive decoding baselines: VCD [19] and M3ID [9]. Moreover, RITUAL is shown to be compatible with both VCD and M3ID, leading to further performance improvements in most configurations. VCD and M3ID are reproduced within our evaluation setting.

Furthermore, RITUAL yields further performance improvement when incorporated with contrastive decoding methods (VCD and M3ID), indicating compatibility. This synergy between contrastive decoding, which aims to reduce language biases, and our approach, which captures a broader range of visual contexts through varying fields of view, effectively mitigates object hallucinations.

Model	Method	Object-level		Attribute-level		Total Score
		Existence \uparrow	Count \uparrow	Position \uparrow	Color \uparrow	
LLaVA 1.5 [28]	base	173.75(± 4.79)	121.67(± 12.47)	117.92(± 3.69)	149.17(± 7.51)	562.50(± 3.96)
	VCD	178.75(± 2.50)	126.25(± 10.40)	120.00(± 4.08)	150.83(± 11.01)	575.84(± 9.67)
	M3ID	177.50(± 6.45)	124.17(± 10.93)	120.00(± 7.07)	152.92(± 5.67)	574.59(± 9.75)
	RITUAL	187.50(± 2.89)	139.58(± 7.62)	125.00(± 10.27)	164.17(± 6.87)	616.25(± 20.38)
	RITUAL+VCD	185.00(± 4.08)	140.84(± 4.41)	125.00(± 7.07)	165.83(± 6.46)	616.67(± 11.14)
	RITUAL+M3ID	187.50(± 2.89)	141.25(± 9.85)	125.00(± 10.27)	164.17(± 6.87)	617.92(± 22.12)
InstructBLIP [6]	base	160.42(± 5.16)	79.17(± 8.22)	79.58(± 8.54)	130.42(± 17.34)	449.58(± 24.09)
	VCD	158.75(± 7.25)	90.75(± 3.11)	70.00(± 15.81)	132.50(± 18.78)	452.00(± 31.57)
	M3ID	158.33(± 5.44)	94.58(± 9.85)	72.50(± 17.03)	128.33(± 14.72)	453.75(± 26.82)
	RITUAL	182.50(± 6.45)	74.58(± 5.99)	67.08(± 10.31)	139.17(± 0.96)	463.33(± 12.40)
	RITUAL+VCD	185.00(± 4.08)	75.00(± 7.07)	62.50(± 6.46)	141.67(± 6.53)	464.17(± 9.07)
	RITUAL+M3ID	182.50(± 6.45)	74.58(± 2.84)	63.33(± 11.55)	140.42(± 2.10)	460.83(± 11.11)

Table 2: **Results on MME-Hallucination [10].** RITUAL effectively mitigates hallucinations at both the object and attribute levels, outperforming contrastive decoding methods [9, 19] in Total Score.

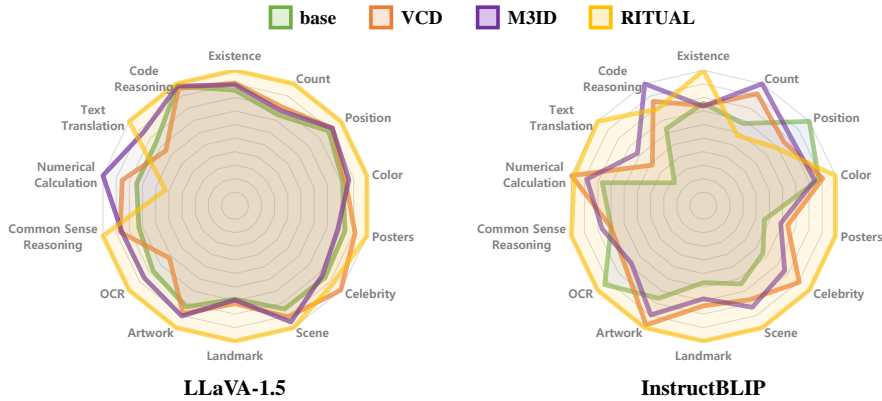


Figure 4: **Comparison on MME-Fullset [10].** When equipped with RITUAL, LLaVA-1.5 [28] performs best in 12 out of 14 categories, while InstructBLIP [6] excels in 11 categories. RITUAL not only reduces hallucinations but also enhances the general capabilities of LVLMs.

Results on MME-Hallucination. In Table 2, we compare the results on the MME-hallucination subset [10] to verify the model’s effectiveness in reducing various types of hallucinations beyond object existence. When combined with LLaVA-1.5 [28], RITUAL outperforms all counterparts across both object-level (Existence and Count) and attribute-level (Position and Color) evaluations. With InstructBLIP [6], while M3ID [9] shows a slight advantage in Count and Position, RITUAL surpasses the baseline and other contrastive decoding methods in the total score. Moreover, when combined with existing methods like VCD [19] and M3ID, RITUAL exhibits further performance enhancement. RITUAL exhibits lower performance in Count and Position tasks due to the inherent challenges associated with specific transformations. For instance, tasks like Count may be impacted by cropping transformations that alter the visible quantity of objects, while Position accuracy may be affected by flipping transformations that change the spatial arrangement of objects.

Results on MME-Fullset. As depicted in Fig. 4, we evaluate the MME-Fullset [10] to assess the impact of decoding methods on the general ability of LVLMs. VCD and M3ID show improvements in certain tasks, with VCD excelling in object-level metrics and M3ID in reasoning and attribute-level metrics. Across 14 categories, both LLaVA-1.5 and InstructBLIP adopting RITUAL consistently achieve the highest scores across most tasks, demonstrating its effectiveness of RITUAL in improving visual and textual understanding. By enriching the model’s visual capacity from diverse visual contexts, RITUAL provides a balanced enhancement across a wide range of tasks, making it a versatile and robust method for improving LVM performance. Despite these advancements, some tasks may still exhibit lower performance due to the inherent challenges of statistical bias and language priors affecting LVLMs. Detailed results are in Appendix D.3.

Results on CHAIR. Tab. 3 To assess the reduction of object existence hallucination, we use the CHAIR metrics, where the presence of objects in the description serves as the measurement criterion.

	Method	CHAIR _S ↓	CHAIR _I ↓
LLaVA 1.5 [28]	base	26.2	9.3
	VCD	22.4	7.6
	M3ID	23.0	6.8
	RITUAL	20.6	6.9
	RITUAL+VCD	20.0	6.8
	RITUAL+M3ID	18.0	5.7
InstructBLIP [6]	base	28.6	10.3
	VCD	27.2	9.1
	M3ID	31.8	10.4
	RITUAL	26.0	8.8
	RITUAL+VCD	25.0	8.6
	RITUAL+M3ID	23.4	7.9

Table 3: **Results on CHAIR [34] benchmark.** RITUAL significantly reduces object hallucinations in caption generation compared to VCD [19] and M3ID [9]. It can also boost performance when combined with these baselines. The number of *max new tokens* is set to 64.

Method	TP ↑	FP ↓	TN ↑	FN ↓	Acc. ↑
base	1291	267	1233	209	84.13
VCD	1331(+40)	270(+3)	1230(-3)	169(-40)	85.37
M3ID	1309(+18)	229(-38)	1271(+38)	191(-18)	86.00
RITUAL	1326(+35)	160(-107)	1340(+107)	174(-35)	88.87
RITUAL+VCD	1323(+32)	154(-113)	1346(+113)	177(-32)	89.07
RITUAL+M3ID	1319(+28)	149(-118)	1351(+118)	181(-28)	89.00

Table 4: **Confusion matrix of LLaVA-1.5 [27] on POPE [24] COCO random.** RITUAL performs the best overall by correctly identifying non-relevant instances.

α	Acc. ↑	Prec. ↑	Rec. ↑	F1 ↑
0 (base)	84.13	82.86	86.07	84.43
0.5	87.73	87.04	88.67	87.85
1	88.00	87.70	88.40	88.05
1.5	88.53	88.74	88.27	88.50
2	88.50	89.05	87.80	88.42
2.5	88.27	88.68	87.73	88.20
3	88.87	89.23	88.40	88.81
3.5	88.67	89.40	87.73	88.56

Table 5: **Ablation of α on POPE [24] COCO random.** Based on the results, we set $\alpha = 3$ as the default.

Given the generative nature of the task, we limit the maximum number of new tokens to 64. As shown in Table 3, our RITUAL outperforms both the baseline and previous contrastive decoding approaches. For LLaVA 1.5, RITUAL achieves CHAIR_S and CHAIR_I scores of 20.6 and 6.9, respectively, significantly surpassing both baseline and VCD. While M3ID shows slightly better performance in CHAIR_I, RITUAL attains comparable scores and markedly excels in CHAIR_I. Similarly, for InstructBLIP, RITUAL achieves the best results with CHAIR_S and CHAIR_I scores of 26.0 and 8.8, respectively. Additionally, when combined with VCD and M3ID, RITUAL further reduces the CHAIR score.

4.3 Analysis

Confusion Matrix POPE COCO Random. To analyze the performance of the model in detail, we report the confusion matrix of LLaVA-1.5 [28] on the POPE [24] COCO random setting in Table 4. Notably, RITUAL demonstrates superior performance by significantly reducing False Positives (FP) and increasing True Negatives (TN) compared to other contrastive decoding methods such as VCD [19] and M3ID [9]. This improvement in correctly identifying non-relevant instances contributes to the highest accuracy among all methods. Detailed results for all settings can be found in the Appendix D.4.

Effect of α in RITUAL As shown in Table 5, we conduct an ablation study on the hyperparameter α in Eq. (4), which adjusts the ratio between the output logits of the model conditioned on the original image \mathcal{V} and the transformed image $\mathcal{V}^{(T)}$. We vary α from 0 (standard decoding) to 3.5 on the POPE COCO random setting. Our method consistently outperforms the baseline across a broad spectrum of α values, with accuracy improvement ranging from +3.60 to +4.74. This demonstrates that our approach is robust and effective regardless of the specific hyperparameter value chosen. Based on these results, we set $\alpha = 3$ as the default value.

Qualitative results on LLaVA-Bench. Fig. 5 presents two samples from the LLaVA-Bench [28] with LLaVA-1.5 [28], highlighting the differences between sentences generated by standard decoding (Base) and those produced by RITUAL. The results demonstrate that standard decoding often results in hallucinations, which can be effectively rectified by implementing RITUAL. For instance, in the left-hand image, the baseline model incorrectly identifies a 'street vendor' and 'initiative signs', neither of which are present in the image. Additionally, it misinterprets 'ironing' as 'doing laundry'. In the right-hand image, the baseline model hallucinates objects not present in the image, such as a 'hat', 'paint mustache', and 'two more dogs'. In contrast, our approach helps counteract these hallucinations, generating sentences that reflect a more accurate comprehension of the image.

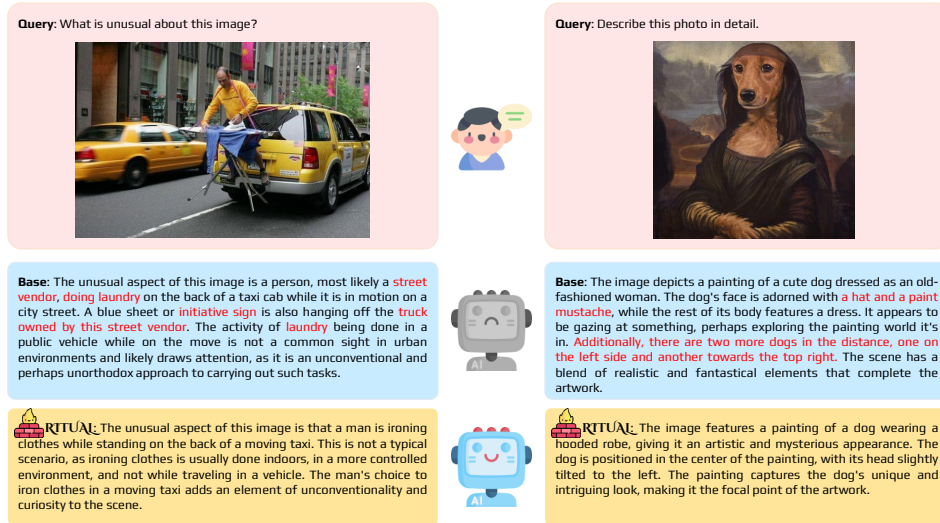


Figure 5: Results on LLaVA-Bench [28]. Hallucinations are highlighted in red. RITUAL well understands ambiguous images and effectively mitigates hallucinations in textual outputs.

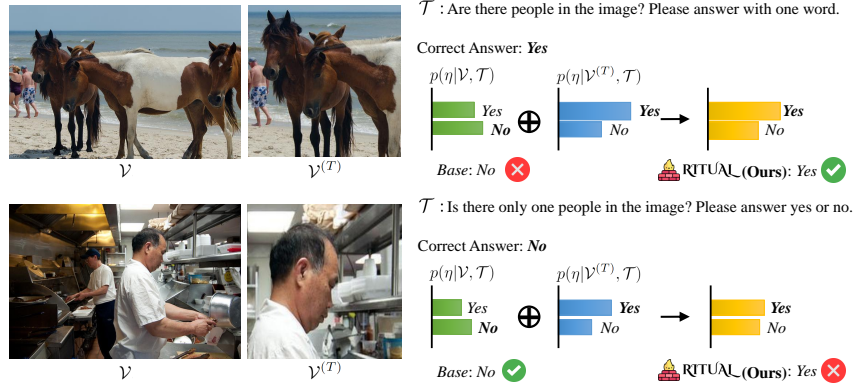


Figure 6: Case study on Crop image transformation. Performance can be affected by the cropping area. Due to the randomness of the selected region, it may sometimes lead to poor outcomes.

5 Discussion

In this study, we have introduces RITUAL, a simple approach aimed at enhancing the reliability of LVLMs. We found that while relying solely on random image transformations can degrade performance, they contribute to mitigating hallucination when used in combination with the original image. Inspired by these findings, RITUAL employs random image transformations to provide LVLMs with a broader visual context, thereby improving the model's robustness against hallucinatory outputs. RITUAL significantly outperforms existing approaches on multiple hallucination benchmarks without requiring additional model training or complex external mechanisms. Moreover, RITUAL is also compatible with existing contrastive decoding techniques, further enhancing performance.

Case Study & Limitations. As shown in Fig. 6, the effectiveness of specific transformations, such as Crop, can depend heavily on the nature of the query. Crop might adjust the position of critical spatial regions, enhancing relevance in the above case while detracting from it in the below case. To illustrate this point, while certain transformations might excel under particular conditions, their efficacy can diminish in others. To mitigate this variability, we opt for a randomized selection from a pool of transformations, allowing for a broader range of adaptability across different image and query contexts. Recognizing the need for a more tailored approach, we introduce a self-feedback mechanism, RITUAL $_{\pm}$, which dynamically selects image transformations that are aware of the image-query context. This method demonstrates a modest improvement in performance by aligning transformations more closely with the specifics of each query, as detailed in Appendix D.2. In future work, we aim to develop a more sophisticated mechanism that can more effectively determine the most suitable transformations based on the interplay between the image and its associated query.³

³Additional case studies can be found in Appendix D.5.

References

- [1] Jinze Bai, Shuai Bai, Shusheng Yang, Shijie Wang, Sinan Tan, Peng Wang, Junyang Lin, Chang Zhou, and Jingren Zhou. Qwen-vl: A versatile vision-language model for understanding, localization, text reading, and beyond. 2023.
- [2] Tim Brooks, Bill Peebles, Connor Holmes, Will DePue, Yufei Guo, Li Jing, David Schnurr, Joe Taylor, Troy Luhman, Eric Luhman, Clarence Ng, Ricky Wang, and Aditya Ramesh. Video generation models as world simulators. 2024.
- [3] Keqin Chen, Zhao Zhang, Weili Zeng, Richong Zhang, Feng Zhu, and Rui Zhao. Shikra: Unleashing multimodal llm’s referential dialogue magic. *arXiv preprint arXiv:2306.15195*, 2023.
- [4] Wei-Lin Chiang, Zhuohan Li, Zi Lin, Ying Sheng, Zhanghao Wu, Hao Zhang, Lianmin Zheng, Siyuan Zhuang, Yonghao Zhuang, Joseph E Gonzalez, et al. Vicuna: An open-source chatbot impressing gpt-4 with 90%* chatgpt quality. See <https://vicuna.lmsys.org> (accessed 14 April 2023), 2(3):6, 2023.
- [5] Yung-Sung Chuang, Yujia Xie, Hongyin Luo, Yoon Kim, James Glass, and Pengcheng He. Dola: Decoding by contrasting layers improves factuality in large language models. *arXiv preprint arXiv:2309.03883*, 2023.
- [6] Wenliang Dai, Junnan Li, Dongxu Li, Anthony Meng Huat Tiong, Junqi Zhao, Weisheng Wang, Boyang Li, Pascale N Fung, and Steven Hoi. Instructblip: Towards general-purpose vision-language models with instruction tuning. *Advances in Neural Information Processing Systems*, 36, 2024.
- [7] Ailin Deng, Zhirui Chen, and Bryan Hooi. Seeing is believing: Mitigating hallucination in large vision-language models via clip-guided decoding. *arXiv preprint arXiv:2402.15300*, 2024.
- [8] Alexey Dosovitskiy, Lucas Beyer, Alexander Kolesnikov, Dirk Weissenborn, Xiaohua Zhai, Thomas Unterthiner, Mostafa Dehghani, Matthias Minderer, Georg Heigold, Sylvain Gelly, et al. An image is worth 16x16 words: Transformers for image recognition at scale. *arXiv preprint arXiv:2010.11929*, 2020.
- [9] Alessandro Favero, Luca Zancato, Matthew Trager, Siddharth Choudhary, Pramuditha Perera, Alessandro Achille, Ashwin Swaminathan, and Stefano Soatto. Multi-modal hallucination control by visual information grounding. *arXiv preprint arXiv:2403.14003*, 2024.
- [10] Chaoyou Fu, Peixian Chen, Yunhang Shen, Yulei Qin, Mengdan Zhang, Xu Lin, Jinrui Yang, Xiawu Zheng, Ke Li, Xing Sun, Yunsheng Wu, and Rongrong Ji. Mme: A comprehensive evaluation benchmark for multimodal large language models. *arXiv preprint arXiv:2306.13394*, 2024.
- [11] Anisha Gunjal, Jihan Yin, and Erhan Bas. Detecting and preventing hallucinations in large vision language models. *arXiv preprint arXiv:2308.06394*, 2023.
- [12] Md Zahid Hasan, Jiajing Chen, Jiyang Wang, Mohammed Shaiqur Rahman, Ameiya Joshi, Senem Velipasalar, Chinmay Hegde, Anuj Sharma, and Soumik Sarkar. Vision-language models can identify distracted driver behavior from naturalistic videos. *IEEE Transactions on Intelligent Transportation Systems*, 2024.
- [13] Ari Holtzman, Jan Buys, Li Du, Maxwell Forbes, and Yejin Choi. The curious case of neural text degeneration. *arXiv preprint arXiv:1904.09751*, 2019.
- [14] Qidong Huang, Xiaoyi Dong, Pan Zhang, Bin Wang, Conghui He, Jiaqi Wang, Dahua Lin, Weiming Zhang, and Nenghai Yu. Opera: Alleviating hallucination in multi-modal large language models via over-trust penalty and retrospection-allocation. *arXiv preprint arXiv:2311.17911*, 2023.
- [15] Drew A Hudson and Christopher D Manning. Gqa: A new dataset for real-world visual reasoning and compositional question answering. In *Proceedings of the IEEE/CVF conference on computer vision and pattern recognition*, pages 6700–6709, 2019.
- [16] Chaoya Jiang, Haiyang Xu, Mengfan Dong, Jiaying Chen, Wei Ye, Ming Yan, Qinghao Ye, Ji Zhang, Fei Huang, and Shikun Zhang. Hallucination augmented contrastive learning for multimodal large language model. *arXiv preprint arXiv:2312.06968*, 2023.
- [17] Junho Kim, Yeon Ju Kim, and Yong Man Ro. What if...?: Counterfactual inception to mitigate hallucination effects in large multimodal models. *arXiv preprint arXiv:2403.13513*, 2024.
- [18] Seongyun Lee, Sue Hyun Park, Yongrae Jo, and Minjoon Seo. Volcano: mitigating multimodal hallucination through self-feedback guided revision. *arXiv preprint arXiv:2311.07362*, 2023.

- [19] Sicong Leng, Hang Zhang, Guanzheng Chen, Xin Li, Shijian Lu, Chunyan Miao, and Lidong Bing. Mitigating object hallucinations in large vision-language models through visual contrastive decoding. *arXiv preprint arXiv:2311.16922*, 2023.
- [20] Junnan Li, Dongxu Li, Silvio Savarese, and Steven Hoi. Blip-2: Bootstrapping language-image pre-training with frozen image encoders and large language models. In *International conference on machine learning*, pages 19730–19742. PMLR, 2023.
- [21] Wei Li, Zhen Huang, Houqiang Li, Le Lu, Yang Lu, Xinmei Tian, Xu Shen, and Jieping Ye. Visual evidence prompting mitigates hallucinations in multimodal large language models. 2023.
- [22] Xiang Lisa Li, Ari Holtzman, Daniel Fried, Percy Liang, Jason Eisner, Tatsunori Hashimoto, Luke Zettlemoyer, and Mike Lewis. Contrastive decoding: Open-ended text generation as optimization. *arXiv preprint arXiv:2210.15097*, 2022.
- [23] Yanze Li, Wenhua Zhang, Kai Chen, Yanxin Liu, Pengxiang Li, Ruiyuan Gao, Lanqing Hong, Meng Tian, Xinhai Zhao, Zhenguo Li, et al. Automated evaluation of large vision-language models on self-driving corner cases. *arXiv preprint arXiv:2404.10595*, 2024.
- [24] Yifan Li, Yifan Du, Kun Zhou, Jinpeng Wang, Wayne Xin Zhao, and Ji-Rong Wen. Evaluating object hallucination in large vision-language models. *arXiv preprint arXiv:2305.10355*, 2023.
- [25] Tsung-Yi Lin, Michael Maire, Serge Belongie, James Hays, Pietro Perona, Deva Ramanan, Piotr Dollár, and C Lawrence Zitnick. Microsoft coco: Common objects in context. In *Computer Vision—ECCV 2014: 13th European Conference, Zurich, Switzerland, September 6–12, 2014, Proceedings, Part V 13*, pages 740–755. Springer, 2014.
- [26] Fuxiao Liu, Kevin Lin, Linjie Li, Jianfeng Wang, Yaser Yacoob, and Lijuan Wang. Mitigating hallucination in large multi-modal models via robust instruction tuning. In *The Twelfth International Conference on Learning Representations*, 2023.
- [27] Haotian Liu, Chunyuan Li, Yuheng Li, and Yong Jae Lee. Improved baselines with visual instruction tuning. *arXiv preprint arXiv:2310.03744*, 2023.
- [28] Haotian Liu, Chunyuan Li, Qingyang Wu, and Yong Jae Lee. Visual instruction tuning. *Advances in neural information processing systems*, 36, 2023.
- [29] Junling Liu, Ziming Wang, Qichen Ye, Dading Chong, Peilin Zhou, and Yining Hua. Qilin-med-vl: Towards chinese large vision-language model for general healthcare. *arXiv preprint arXiv:2310.17956*, 2023.
- [30] Jiaying Lu, Jinneng Rao, Kezhen Chen, Xiaoyuan Guo, Yawen Zhang, Baochen Sun, Carl Yang, and Jie Yang. Evaluation and enhancement of semantic grounding in large vision-language models. In *AAAI-RelLM Workshop*, 2024.
- [31] OpenAI. Chatgpt interaction. Personal communication, 2023.
- [32] Adam Paszke, Sam Gross, Francisco Massa, Adam Lerer, James Bradbury, Gregory Chanan, Trevor Killeen, Zeming Lin, Natalia Gimelshein, Luca Antiga, et al. Pytorch: An imperative style, high-performance deep learning library. *Advances in neural information processing systems*, 32, 2019.
- [33] Alec Radford, Jong Wook Kim, Chris Hallacy, Aditya Ramesh, Gabriel Goh, Sandhini Agarwal, Girish Sastry, Amanda Askell, Pamela Mishkin, Jack Clark, et al. Learning transferable visual models from natural language supervision. In *International conference on machine learning*, pages 8748–8763. PMLR, 2021.
- [34] Anna Rohrbach, Lisa Anne Hendricks, Kaylee Burns, Trevor Darrell, and Kate Saenko. Object hallucination in image captioning. *arXiv preprint arXiv:1809.02156*, 2018.
- [35] Dustin Schwenk, Apoorv Khandelwal, Christopher Clark, Kenneth Marino, and Roozbeh Mottaghi. A-okvqa: A benchmark for visual question answering using world knowledge. In *European Conference on Computer Vision*, pages 146–162. Springer, 2022.
- [36] Zhiqing Sun, Sheng Shen, Shengcao Cao, Haotian Liu, Chunyuan Li, Yikang Shen, Chuang Gan, Liang-Yan Gui, Yu-Xiong Wang, Yiming Yang, et al. Aligning large multimodal models with factually augmented rlhf. *arXiv preprint arXiv:2309.14525*, 2023.
- [37] Gemini Team, Rohan Anil, Sebastian Borgeaud, Yonghui Wu, Jean-Baptiste Alayrac, Jiahui Yu, Radu Soricut, Johan Schalkwyk, Andrew M Dai, Anja Hauth, et al. Gemini: a family of highly capable multimodal models. *arXiv preprint arXiv:2312.11805*, 2023.

- [38] David Wan, Jaemin Cho, Elias Stengel-Eskin, and Mohit Bansal. Contrastive region guidance: Improving grounding in vision-language models without training. *arXiv preprint arXiv:2403.02325*, 2024.
- [39] Bin Wang, Fan Wu, Xiao Han, Jiahui Peng, Huaping Zhong, Pan Zhang, Xiaoyi Dong, Weijia Li, Wei Li, Jiaqi Wang, et al. Vigc: Visual instruction generation and correction. *arXiv preprint arXiv:2308.12714*, 2023.
- [40] Junyang Wang, Yuhang Wang, Guohai Xu, Jing Zhang, Yukai Gu, Haitao Jia, Ming Yan, Ji Zhang, and Jitao Sang. Amber: An llm-free multi-dimensional benchmark for mllms hallucination evaluation. *arXiv preprint arXiv:2311.07397*, 2023.
- [41] Xintong Wang, Jingheng Pan, Liang Ding, and Chris Biemann. Mitigating hallucinations in large vision-language models with instruction contrastive decoding. *arXiv preprint arXiv:2403.18715*, 2024.
- [42] Sam Wiseman and Alexander M Rush. Sequence-to-sequence learning as beam-search optimization. *arXiv preprint arXiv:1606.02960*, 2016.
- [43] Peng Wu, Xuerong Zhou, Guansong Pang, Lingru Zhou, Qingsen Yan, Peng Wang, and Yanning Zhang. Vadclip: Adapting vision-language models for weakly supervised video anomaly detection. In *Proceedings of the AAAI Conference on Artificial Intelligence*, volume 38, pages 6074–6082, 2024.
- [44] Dingchen Yang, Bowen Cao, Guang Chen, and Changjun Jiang. Pensieve: Retrospect-then-compare mitigates visual hallucination. *arXiv preprint arXiv:2403.14401*, 2024.
- [45] Shukang Yin, Chaoyou Fu, Sirui Zhao, Tong Xu, Hao Wang, Dianbo Sui, Yunhang Shen, Ke Li, Xing Sun, and Enhong Chen. Woodpecker: Hallucination correction for multimodal large language models. *arXiv preprint arXiv:2310.16045*, 2023.
- [46] Tianyu Yu, Yuan Yao, Haoye Zhang, Taiwen He, Yifeng Han, Ganqu Cui, Jinyi Hu, Zhiyuan Liu, Hai-Tao Zheng, Maosong Sun, et al. Rlhf-v: Towards trustworthy mllms via behavior alignment from fine-grained correctional human feedback. *arXiv preprint arXiv:2312.00849*, 2023.
- [47] Zihao Yue, Liang Zhang, and Qin Jin. Less is more: Mitigating multimodal hallucination from an eos decision perspective, 2024.
- [48] Bohan Zhai, Shijia Yang, Chenfeng Xu, Sheng Shen, Kurt Keutzer, Chunyuan Li, and Manling Li. Halle-control: Controlling object hallucination in large multimodal models, 2024.
- [49] Yi-Fan Zhang, Weichen Yu, Qingsong Wen, Xue Wang, Zhang Zhang, Liang Wang, Rong Jin, and Tieniu Tan. Debiasing large visual language models. *arXiv preprint arXiv:2403.05262*, 2024.
- [50] Linxi Zhao, Yihe Deng, Weitong Zhang, and Quanquan Gu. Mitigating object hallucination in large vision-language models via classifier-free guidance. *arXiv preprint arXiv:2402.08680*, 2024.
- [51] Zhiyuan Zhao, Bin Wang, Linke Ouyang, Xiaoyi Dong, Jiaqi Wang, and Conghui He. Beyond hallucinations: Enhancing lvlms through hallucination-aware direct preference optimization. *arXiv preprint arXiv:2311.16839*, 2023.
- [52] Hongjian Zhou, Boyang Gu, Xinyu Zou, Yiru Li, Sam S Chen, Peilin Zhou, Junling Liu, Yining Hua, Chengfeng Mao, Xian Wu, et al. A survey of large language models in medicine: Progress, application, and challenge. *arXiv preprint arXiv:2311.05112*, 2023.
- [53] Yiyang Zhou, Chenhang Cui, Jaehong Yoon, Linjun Zhang, Zhun Deng, Chelsea Finn, Mohit Bansal, and Huaxiu Yao. Analyzing and mitigating object hallucination in large vision-language models. *arXiv preprint arXiv:2310.00754*, 2023.
- [54] Deyao Zhu, Jun Chen, Xiaoqian Shen, Xiang Li, and Mohamed Elhoseiny. Minigt-4: Enhancing vision-language understanding with advanced large language models. *arXiv preprint arXiv:2304.10592*, 2023.

Appendix

A Detailed Experimental Settings

POPE⁴

We utilize the official benchmark from [24], which includes 3,000 question-answer pairs for each of the random, popular, and adversarial settings. We use the query template 'Is there a [object] in the image?'. Here, [object] is selected randomly, from the most frequent objects in the dataset, or from objects that frequently co-occur with [object], corresponding to the random, popular, and adversarial settings respectively. We evaluate the performance based on whether the model-generated output contained the ground truth ('Yes' or 'No') using accuracy, precision, recall, and average F1-score.

MME⁵

The MME [10] dataset consists of 10 perception categories (existence, count, position, color, posters, celebrity, scene, landmark, artwork, OCR) and 4 recognition ones (commonsense reasoning, numerical calculation, text translation, code reasoning). Each query is used with an image-related question followed by 'Please answer yes or no.' We report the sum of accuracy at the query level and image level following the official implementation.

CHAIR⁶

We select 500 random images from the COCO [25] validation set and generate the output using the query "Please Describe this image in detail.". Due to the computational complexity, we restrict the *max new tokens* to 64. Following the M3ID [9], we report two assessment metrics, C_s and C_i , which calculate the hallucination ratio per sentence and instance as follows:

$$C_s = \frac{|\{\text{sentences with hallucinated objects}\}|}{|\{\text{all sentences}\}|}, C_i = \frac{|\{\text{hallucinated objects}\}|}{|\{\text{all objects mentioned}\}|}. \quad (5)$$

LLaVA-Bench⁷

The LLaVA-Bench [28] dataset consists of 24 images along with 60 image-related questions. This dataset is demanding as it has been collected from a variety of domains including diverse scenes, memes, paintings, sketches, and more. We conduct qualitative case studies on this dataset to exhibit the efficacy of RITUA in challenging tasks and its adaptability to new domains.

B License of Assets

POPE [24] is licensed under MIT License. CHAIR [34] is made available under the BSD 2-Clause License. LLaVA-Bench is available under Apache-2.0 License.

LLaVA [28] is licensed under the Apache-2.0 License. InstructBLIP [6] is under BSD-3-Clause License.

PyTorch [32] is released under the Modified BSD License.

C Further Implementation Details

C.1 Image Transformation

We set predefined six commonly used image transformations and randomly applied one of them for each image. We provide a concise description and implementation details below. We employ the Pytorch/Torchvision [32] implementation for transformation.

Horizontal flip. Flip the image in the horizontal direction.

⁴<https://github.com/RUCAIBox/POPE>

⁵<https://github.com/BradyFU/Awesome-Multimodal-Large-Language-Models/tree/Evaluation>

⁶<https://github.com/LisaAnne/Hallucination>

⁷<https://huggingface.co/datasets/liuhaotian/llava-bench-in-the-wild>

Vertical flip. Flip the image in the vertical direction.

Rotate. Rotate the image by angle. We set $degrees=(-180, +180)$.

Color jitter. Change the brightness, contrast, saturation, and hue of an image. We set $brightness=1$, $contrast=1$, $saturation=1$, $hue=0.5$.

Gaussian blur. Blurs image with randomly chosen Gaussian blur. We set $kernel_size=13$ and $sigma=(1.5, 2.0)$.

Crop. Crop a random portion of an image and resize it to a given size. We set $size=336$ as the same as the original data resize scale.

C.2 Decoding Methods

For a fair comparison, we adopt adaptive plausible constraint based on the confidence level related to the output distribution from the original visual inputs following [19, 22].

$$\mathcal{O}(\eta_{<t}) = \{\eta_t \in \mathcal{O} : p_\theta(\eta_t | \mathcal{V}, \mathcal{T}, \eta_{<t}) \geq \beta \max_w p_\theta(w | v, x, y_{<t})\}. \quad (6)$$

where \mathcal{O} is the output vocabulary of LVLMM, and β is a plausible constraint parameter hyperparameter that adjusts the truncation of the next token distribution. The logits of tokens not in \mathcal{O} are set $-\infty$ so that larger β results in retaining only tokens with higher probabilities. We set $\beta=0.1$ for all experiments. We configured the hyperparameter with a value of $\alpha=3$ in Eq. (4) by default. Note that we reproduced VCD [19] and M3ID [9] with our settings. We use the contrastive distribution of VCD as shown in Eq. (7) and set the balancing parameter $\gamma=2$ and $\delta=1$, and the total noise step = 500 for generating the corrupted image \mathcal{V}' .

$$\eta_t^{VCD} \sim \gamma p_\theta(\eta_t | \mathcal{V}, \mathcal{T}, \eta_{<t}) - \delta p_\theta(\eta_t | \mathcal{V}', \mathcal{T}, \eta_{<t}). \quad (7)$$

Furthermore, we reproduced a key concept of M3ID, preventing conditioning dilution by introducing the unconditioned model as below:

$$\eta_t^{M3ID} \sim p_\theta(\eta_t | \mathcal{V}, \mathcal{T}, \eta_{<t}) + \frac{1 - e^{-\lambda t}}{e^{-\lambda t}} (p_\theta(\eta_t | \mathcal{V}, \mathcal{T}, \eta_{<t}) - p_\theta(\eta_t | \mathcal{T}, \eta_{<t})) \quad (8)$$

We set the λ , balancing parameter between conditioned model and unconditioned model, to 0.1. Note that $\eta_t^{Transformed} = p_\theta(\eta_t | \mathcal{V}^{(T)}, \mathcal{T}, \eta_{<t})$. When we use RITUAL and contrastive decoding, we used combined distribution as $\zeta \eta_t^{Transformed} + \eta_t^D$ where $\{VCD, M3ID\} \in D$. In this case, we set $\gamma=1$, $\delta=0.1$, and $\zeta=3$ for RITUAL+VCD, and $\lambda=0.1$ and $\zeta=3.5$ for RITUAL+M3ID. The code is implemented in Python 3.10 with PyTorch 2.0.1 [32], and all experiments are conducted utilizing an NVIDIA RTX 3090 GPU.

D Additional Experiments

D.1 Random Image Transformation vs. Single Image Transformation

In our study, we randomly choose one of six image transformation techniques (horizontal flip, vertical flip, rotate, color jitter, Gaussian blur, and crop) for the transformed image $\mathcal{V}^{(T)}$. We compared the results with a method that only adopts specific transformations rather than making a random choice. As illustrated in Table 6, our analysis revealed that the effectiveness of each augmentation varied depending on the dataset setup. For instance, employing solely color jitter led to the best results in the popular setup, while it delivered the poorest outcomes in the adversarial setup. Reviewing Figure 3, it becomes evident that the same transformation may have varying effects, beneficial or detrimental, based on the specific image and query. Therefore, we have chosen to use random selection as our primary method.

D.2 Self-feedback for Transformation Selection

As we mentioned in Sec. 5 and Appendix D.1, transformation may interfere with the model’s accurate predictions. To address this issue, we implemented a simple mechanism that allows the model to select an image-query-aware transformation through self-feedback. As depicted in Fig. 7, the model

System Prompt

A chat between a curious human and an artificial intelligence assistant. The assistant gives helpful, detailed, and polite answers to the human's questions.

Image

{image sample}

Query

{query sample}

Instruction

You are an image augmentation evaluator. Your task is to evaluate the impact of different image augmentation techniques on question-answering task related those images. Here is the list of augmentations you need to examine:

1. Horizontal flip
 - Description: Reflects the image along a vertical axis, which means that the left side of the image becomes the right side, and vice versa, while the top and bottom remain unchanged.
 - Pros: Can offer a different perspective without changing the semantic meaning of the content.
 - Cons: May cause issues like text becoming unreadable or objects appearing in the wrong direction.
2. Vertical flip
 - Description: Flips the image along a horizontal axis, creating an upside-down version while maintaining left-right orientation.
 - Pros: Useful for certain artistic effects or when orientation is not critical.
 - Cons: May result in unnatural-looking images, especially if the flipped orientation affects the logic of the scene, such as objects appearing in physically impossible orientations.
3. Rotation
 - Description: Alters the image orientation by a certain angle.
 - Pros: Enables viewing images from different angles.
 - Cons: May distort image content at extreme angles, potentially leading to the loss of important features.
4. Color jitter
 - Description: Introduces variations in color, including brightness, contrast, saturation, and hue.
 - Pros: Useful for simulating different lighting conditions or color variations in images.
 - Cons: May introduce unrealistic colors or distortions, which can be problematic for tasks where color information is critical.
5. Gaussian blur
 - Description: Applies a smoothing effect, reducing noise and fine detail.
 - Pros: Helps in noise reduction and focusing on more prominent features.
 - Cons: May remove important details, not suitable for tasks where fine details are crucial.
6. Crop
 - Description: Removes parts of the image, focusing on a specific region of interest.
 - Pros: Helps in emphasizing relevant parts of the image, potentially reducing irrelevant information.
 - Cons: May remove important context or details necessary for a comprehensive understanding the image.

Consider the impact of each augmentation on the understanding of an image when answering questions. Select the most positive augmentation that helps answer questions more accurately.

Answer always in the following form:
[Number]. [Most beneficial augmentation]

For example:
1. Horizontal flip

Figure 7: Prompt for RITUAL+.

Setup	Transformation	LLaVA 1.5 [28]				
		Acc. \uparrow	Prec. \uparrow	Rec. \uparrow	F1 \uparrow	
MS-COCO [25]	Random	Horizontal Flip	89.50	89.95	88.93	89.44
		Vertical Flip	88.60	88.76	88.40	88.58
		Rotate	88.90	89.56	88.07	88.81
		Color Jitter	88.83	89.98	87.40	88.67
		Gaussian Blur	88.77	89.48	87.87	88.66
		Crop	88.47	89.36	87.33	88.33
		Random Selection	88.87	89.23	88.40	88.58
	Popular	Horizontal Flip	85.60	83.21	89.20	86.10
		Vertical Flip	85.23	83.05	88.53	85.71
		Rotate	86.20	84.67	88.40	86.50
		Color Jitter	86.20	84.90	88.07	86.45
		Gaussian Blur	84.93	83.29	87.40	85.30
		Crop	85.70	84.62	87.27	85.92
		Random Selection	85.83	84.17	88.27	86.17
	Adversarial	Horizontal Flip	79.50	74.65	89.33	81.34
		Vertical Flip	79.10	74.65	88.13	80.83
		Rotate	79.73	75.06	89.07	81.46
		Color Jitter	78.70	74.47	87.33	80.39
Gaussian Blur		78.73	74.19	88.13	80.56	
Crop		79.37	75.48	87.00	80.83	
Random Selection		78.80	74.43	87.73	80.54	

Table 6: Comparison of single image transformation vs. random image transformation.

MS-COCO [25]	Method	LLaVA 1.5 [28]			
		Acc. \uparrow	Prec. \uparrow	Rec. \uparrow	F1 \uparrow
Random	<i>base</i>	84.13	82.86	86.07	84.43
	RITUAL	88.87	89.23	88.40	88.81
	RITUAL+	89.17	88.89	89.53	89.21
Popular	<i>base</i>	80.87	78.23	85.53	81.72
	RITUAL	85.83	84.17	88.27	86.17
	RITUAL+	85.40	83.27	88.60	85.85
Adversarial	<i>base</i>	76.23	71.75	86.53	78.45
	RITUAL	78.80	74.43	87.73	80.54
	RITUAL+	79.17	74.48	88.73	80.99

Table 7: Effect of self-feedback on transformation selection. While, RITUAL randomly selects image transformations, RITUAL+ selects image transformation via self-feedback from LVLMS.

receives an image-question pair along with a comprehensive description of transformations, after which it selects the most suitable transformation in a self-feedback manner. Note that RITUAL+ is the model with self-feedback transformation selection rather than random choice. We compared the performance between RITUAL and RITUAL+ on POPE COCO setups in Table 7. RITUAL+ declines in the popular setting while it achieves performance improvement in random and adversarial setups. Considering the computational complexity involved in the self-feedback process, the potential for performance improvement appears limited, suggesting the need for more advanced methodologies.

D.3 Detailed Results on MME-Fullset

We present the detailed performance on MME-Fullset in Table 8. RITUAL exhibits significant performance improvement in both LLaVA-1.5 and InstructBLIP across various perception and recognition tasks in most cases. These results underscore the effectiveness of RITUAL in handling diverse tasks, including beyond the hallucination mitigation, showcasing its potential to enhance LVLMS’ ability to accurately interpret and analyze visual content. However, it is important to acknowledge that RITUAL’s performance in the count, position, numerical calculation, and code reasoning categories does not currently match the levels achieved in the other tasks. In the same way as shown in Fig. 6, some transformations may not suit the query and could actually contribute to

Task	Category	LLaVA 1.5 [28]				Instructblip [6]				
		base	VCD	M3ID	RITUAL	base	VCD	M3ID	RITUAL	
Perception	Existence	173.75 (±4.79)	178.75 (±2.5)	177.5 (±6.45)	187.50 (±2.89)	160.42 (±5.16)	158.75 (±7.25)	158.33 (±5.44)	182.50 (±6.45)	
	Count	121.67 (±12.47)	126.25 (±10.4)	124.17 (±10.93)	139.58 (±7.62)	79.17 (±8.22)	90.75 (±3.11)	94.58 (±9.85)	74.58 (±5.99)	
	Position	117.92 (±3.69)	120.00 (±4.08)	120.00 (±7.07)	125.00 (±10.27)	79.58 (±8.54)	70.00 (±15.81)	72.50 (±17.03)	67.08 (±10.31)	
	Color	149.17 (±7.51)	150.83 (±11.01)	152.92 (±5.67)	164.17 (±6.87)	130.42 (±17.34)	132.5 (±18.78)	128.33 (±14.72)	139.17 (±0.96)	
	Posters	124.24 (±3.36)	129.34 (±4.11)	120.49 (±8.23)	135.46 (±0.94)	101.96 (±1.5)	114.29 (±7.07)	110.54 (±0.62)	139.46 (±4.85)	
	Celebrity	115.44 (±3.98)	124.78 (±6.23)	113.9 (±4.85)	120.07 (±1.88)	105.22 (±2.23)	128.31 (±5.14)	119.05 (±5.01)	134.63 (±4.19)	
	Scene	147.44 (±6.26)	152.69 (±2.46)	155.94 (±2.83)	159.75 (±2.79)	130.19 (±3.9)	140.56 (±2.92)	145.31 (±5.78)	158.63 (±2.62)	
	Landmark	133.31 (±4.73)	136.00 (±7.35)	133.81 (±5.84)	157.81 (±2.19)	118.13 (±6.37)	131.06 (±3.71)	127.06 (±7.17)	150.69 (±1.39)	
	Artwork	107.31 (±2.61)	110.50 (±0.79)	111.69 (±0.92)	117.31 (±2.23)	91.44 (±5.61)	102.75 (±4.24)	98.44 (±3.91)	103.94 (±6.95)	
	OCR	107.50 (±13.99)	98.13 (±7.18)	112.50 (±10.21)	121.25 (±6.29)	90.63 (±6.88)	81.25 (±6.61)	78.75 (±17.85)	93.75 (±8.29)	
	Recognition	Commonsense Reasoning	99.82 (±9.39)	108.04 (±2.36)	107.32 (±10.13)	115.54 (±4.92)	92.68 (±8.64)	92.86 (±6.2)	96.43 (±9.7)	109.11 (±8.17)
		Numerical Calculation	60.00 (±12.42)	63.75 (±8.54)	68.75 (±7.22)	52.50 (±8.9)	56.88 (±15.6)	64.38 (±6.25)	60.63 (±19.51)	63.75 (±9.24)
Text Translation		81.88 (±13.13)	77.50 (±8.90)	87.50 (±10.61)	93.75 (±10.51)	56.88 (±17.49)	66.25 (±6.61)	72.50 (±12.75)	89.38 (±12.48)	
Code Reasoning		64.38 (±25.93)	63.75 (±25.86)	64.38 (±25.93)	65.00 (±10.21)	63.75 (±11.27)	72.50 (±20.31)	78.13 (±15.33)	70.00 (±4.08)	

Table 8: Results on MME-Fullset [10].

a decrease in performance. Addressing and surmounting these identified drawbacks represents our primary objective moving forward.

D.4 Confusion Matrices of LLaVA-1.5

We report the confusion matrices in Table 9 for the POPE benchmark. Our method significantly improves True Negatives (TN) while maintaining a similar level of True Positives (TP) compared to existing contrastive decoding methods. It implies that our method achieves the highest accuracy by significantly improving the identification of non-relevant instances compared to the baseline and previous methods.

D.5 More Case Studies

We provide case studies on all benchmarks (POPE [24], MME [10], CHAIR [34], and LLaVA-Bench [28]) to verify the efficacy of RITUAL. Results are shown in Figs. 8 to 11.

E Broader Impacts

The broader impacts of proposed RITUAL have benefits and risks along with its release.

[+] Increased Reliability in Critical Applications. By mitigating hallucinations in LVLMs, we can significantly enhance the reliability of these models in critical applications such as medical diagnosis, autonomous driving, and surveillance. This leads to more accurate and dependable outcomes, which are crucial for safety and effectiveness in these fields.

Setup	Method	LLaVA 1.5 [28]					InstructBLIP [6]					
		TP ↑	FP ↓	TN ↑	FN ↓	Acc. ↑	TP ↑	FP ↓	TN ↑	FN ↓	Acc. ↑	
MS-COCO [25]	Random	<i>base</i>	1291	267	1233	209	84.13	1255	271	1229	245	82.80
		VCD	1331	270	1230	169	85.37	1240	222	1278	260	83.93
		M3ID	1309	229	1271	191	86.00	1260	229	1271	240	84.37
		RITUAL	1326	160	1340	174	88.87	1302	137	1363	198	88.83
		RITUAL+VCD	1323	154	1346	177	89.07	1311	132	1368	189	89.30
		RITUAL+M3ID	1319	149	1351	181	89.00	1294	126	1374	206	88.93
	Popular	<i>base</i>	1283	357	1143	217	80.87	1238	464	1036	262	75.80
		VCD	1306	373	1127	194	81.10	1234	402	1098	266	77.73
		M3ID	1324	339	1161	176	82.83	1259	440	1060	241	77.30
		Ours	1324	249	1251	176	85.83	1309	350	1150	191	81.97
		RITUAL+VCD	1328	255	1245	172	85.77	1309	324	1176	191	82.83
		RITUAL+M3ID	1320	259	1241	180	85.37	1304	347	1153	196	81.90
Adversarial	<i>base</i>	1298	511	989	202	76.23	1263	501	999	237	75.40	
	VCD	1308	540	960	192	75.60	1253	449	1051	247	76.80	
	M3ID	1310	479	1021	190	77.70	1259	478	1022	241	76.03	
	RITUAL	1316	452	1048	184	78.80	1308	446	1054	192	78.73	
	RITUAL+VCD	1323	435	1065	177	79.60	1312	440	1060	188	79.07	
	RITUAL+M3ID	1320	444	1056	180	79.20	1300	432	1068	200	78.93	
A-OKVQA [35]	Random	<i>base</i>	1373	421	1079	127	81.73	1300	366	1134	200	81.13
		VCD	1405	450	1050	95	81.83	1297	337	1163	203	82.00
		M3ID	1407	400	1100	93	83.57	1357	387	1113	143	82.33
		RITUAL	1413	358	1142	87	85.17	1378	264	1236	122	87.17
		RITUAL+VCD	1406	353	1147	94	85.10	1373	270	1230	127	86.77
		RITUAL+M3ID	1419	341	1159	81	85.93	1369	254	1246	131	87.17
	Popular	<i>base</i>	1375	575	925	125	76.67	1303	533	967	197	75.67
		VCD	1393	652	848	107	74.70	1314	519	981	186	76.50
		M3ID	1416	551	949	84	78.83	1375	513	987	125	78.73
		RITUAL	1416	551	949	84	78.83	1375	513	987	125	78.73
		RITUAL+VCD	1414	539	961	86	79.17	1383	518	982	117	78.83
		RITUAL+M3ID	1418	529	971	82	79.63	1373	497	1003	127	79.20
Adversarial	<i>base</i>	1369	847	653	131	67.40	1302	762	738	198	68.00	
	VCD	1400	877	623	100	67.43	1327	707	793	173	70.67	
	M3ID	1404	861	639	96	68.10	1326	739	761	174	69.57	
	RITUAL	1414	857	643	86	68.57	1378	770	730	122	70.27	
	RITUAL+VCD	1412	848	652	88	68.80	1385	755	745	115	71.00	
	RITUAL+M3ID	1415	852	648	85	68.77	1367	788	712	133	69.30	
GQA [15]	Random	<i>base</i>	1390	453	1047	110	81.23	1289	391	1109	211	79.93
		VCD	1426	481	1019	74	81.50	1300	345	1155	200	81.83
		M3ID	1417	432	1068	83	82.83	1315	398	1102	185	80.57
		RITUAL	1435	352	1148	65	86.10	1327	281	1219	173	84.87
		RITUAL+VCD	1435	354	1146	65	86.03	1334	285	1215	166	84.97
		RITUAL+M3ID	1433	344	1156	67	86.30	1322	272	1228	178	85.00
	Popular	<i>base</i>	1402	727	773	98	72.50	1281	599	901	219	72.73
		VCD	1422	775	725	78	71.57	1298	588	912	202	73.67
		M3ID	1410	725	775	90	72.83	1316	579	921	184	74.57
		RITUAL	1435	691	809	65	74.80	1326	591	909	174	74.50
		RITUAL+VCD	1431	679	821	69	75.07	1331	571	929	169	75.33
		RITUAL+M3ID	1433	701	799	67	74.40	1331	564	936	169	75.57
Adversarial	<i>base</i>	1397	868	632	103	67.63	1285	698	802	215	69.57	
	VCD	1413	889	611	87	67.47	1279	696	804	221	69.43	
	M3ID	1417	873	627	83	68.13	1292	725	775	208	68.90	
	RITUAL	1437	890	610	63	68.23	1327	722	778	173	70.17	
	RITUAL+VCD	1435	865	635	65	69.00	1328	721	779	172	70.23	
	RITUAL+M3ID	1429	865	635	71	68.80	1343	713	787	157	71.00	

Table 9: Confusion matrices on POPE [24] benchmark.

[+] Reduction in Misinformation. Reducing hallucinations helps minimize the spread of misinformation in applications like news generation or content moderation, thereby contributing to more accurate and trustworthy information dissemination.

[-] Increased Computational Costs. Implementing our hallucination mitigation technique RITUAL requires two times forward passes, which can lead to increased costs and energy consumption.

Despite the potential negative impacts, the positive aspects of RITUAL far outweigh the drawbacks. Enhancing trustworthiness in LLMs is a crucial issue, and we hope our work stimulates the research community to develop more effective hallucination mitigation strategies to address it.

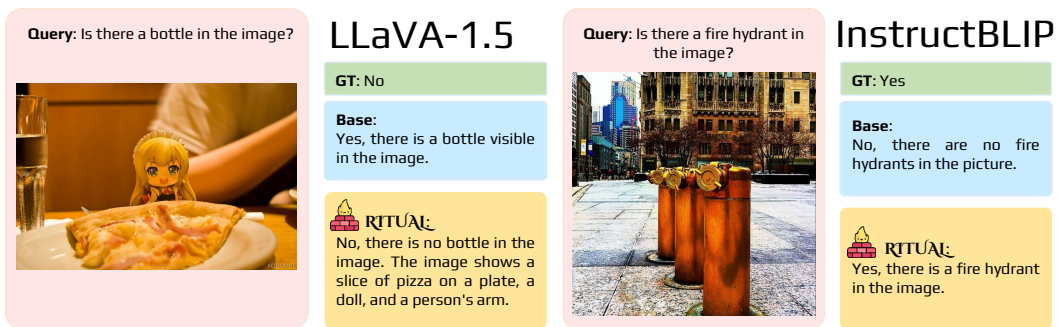


Figure 8: Results on POPE [24].

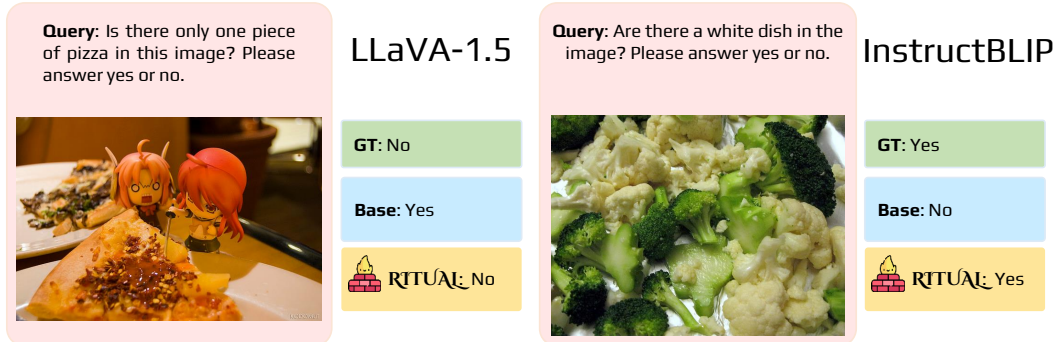


Figure 9: Results on MME [10].

Query: Please describe this image in details.



LLaVA-1.5

Base:

The image depicts a large white moving truck, presumably carrying a delivery of brown bottles, as it either stops or drives down a road. The truck takes up a significant part of the scene, covering more than half of the image. It is parked near the side of a building, with ...



The image features a white truck parked on a street, with a large advertisement for beer displayed on the back of the truck. The truck is positioned near a tree, and there is another truck visible in the background. The advertisement on the truck showcases a variety ...

Query: Please describe this image in details.



InstructBLIP

Base:

The image displays a busy stage at a restaurant or food preparation facility with several chefs or cooks preparing meals. There are nine people present in the room. In addition to the cooks, there is a person observing the work from behind a fence, likely assessing the progress of the ...



The image features a kitchen with a man preparing food in a professional setting. He is standing in front of a counter with a large food processor, which is positioned towards the left side of the scene. The man is wearing a chef's hat and is focused on preparing the food. There ...

Figure 10: Results on CHAIR [34].



Figure 11: Additional case studies of LLaVA-1.5 on LLaVA-Bench [28]. Hallucinations are highlighted in red.